⟲ANS

Check for updates

Simultaneous Measurement of ^{235}U Fission and Capture Cross Sections From 0.01 eV to 3 keV Using a Gamma Multiplicity Detector

Y. Danon,[a*] D. Williams,[a†] R. Bahran,[a‡] E. Blain,[a] B. McDermott,[a] D. Barry,[b] G. Leinweber,[b] R. Block,[b] and M. Rapp[b]

^{a}*Rensselaer Polytechnic Institute, Gaerttner LINAC Center, 110 8th St., Troy, New York 12180*
^{b}*Naval Nuclear Laboratory, P.O. Box 1072, Schenectady, New York 12301-1072*

Abstract — *The neutron microscopic capture cross section for ^{235}U is a critical parameter for the design and operation of nuclear reactors. The evaluated nuclear data libraries of ENDF/B-VII.1 and JENDL-4.0 have nearly identical values for the neutron capture cross section for neutron energies below 0.5 keV. In the most recent release of the JENDL library the onset of the unresolved resonance region was changed from 2.25 keV to 0.5 keV. In the energy region from 1.5 keV to 2.25 keV the average neutron capture cross section from ENDF/B-VII.1 is about 10% higher than that from JENDL-4.0. In an attempt to address the discrepancies between the libraries, a measurement of the neutron capture cross section of ^{235}U was conducted at the Gaerttner LINAC Center located at Rensselaer Polytechnic Institute. This measurement used a 16-segment γ-multiplicity NaI(Tl) detector to detect the prompt gammas emitted from neutron interactions with a highly enriched ^{235}U sample. Using the time-of-flight method, detected events were recorded and grouped based on the total gamma energy per interaction and observed multiplicity. A method was developed to separate fission from capture based on total energy deposition and gamma multiplicity. Application of this method in the thermal and resonance region below 0.5 keV for both the fission and capture produced cross sections that are in good agreement with both ENDF/B-VII.1 and JENDL-4.0 evaluations. The measurements support a lower ^{235}U neutron capture cross section in the energy range 0.5 to 2.25 keV, which is closer to JENDL 4.0.*

Keywords — *Capture, fission, ^{235}U.*

Note — *Some figures may be in color only in the electronic version.*

I. INTRODUCTION

Accurate nuclear data are required to reduce the uncertainty in calculations for nuclear reactor design and criticality safety applications. The improved computing capabilities for reactor calculations have elevated the importance of nuclear data in the calculations. One such example in which more accurate experimental data are needed is the microscopic capture cross section of ^{235}U in the resolved resonance region and in the beginning of the unresolved resonance region (URR). Otuka et al.[1] analyzed several critical benchmarks that were sensitive to kilo-electron-volt neutrons and found that a reduction of the JENDL-3.3 ^{235}U capture cross section was necessary in order to improve the agreement between experiments and calculations. In the most recent release of the JENDL

*E-mail: danony@rpi.edu
†Current address: Defense Threat Reduction Agency, 8725 John J. Kingman Road, Fort Belvoir, Virginia 22060
‡Current address: Los Alamos National Laboratory, Bikini Atoll Road, Los Alamos, New Mexico 87545

library, the onset of the URR was changed from 2.25 keV to 0.5 keV. In this energy region the average neutron capture cross section from ENDF/B-VII.1 (Ref. 2) is about 10% higher than that from JENDL-4.0 (Ref. 3). The JEFF-3.1.1 (Ref. 4) evaluated library is nearly identical to the ENDF/B-VII.1 library in this same region for the neutron capture cross section for ^{235}U. The present measurement of the ^{235}U neutron capture cross section was conducted in an attempt to address the discrepancies between the libraries. Researchers at Los Alamos National Laboratory (LANL) and Lawrence Livermore National Laboratory also identified these discrepancies and conducted a new measurement of the neutron capture cross section of ^{235}U (Ref. 5). Other recent work includes measurements at the nTOF facility[6]; however, it is not clear what the impact of the nTOF measurements is in the energy range in question.

In order to perform this measurement we avoided the standard method of a sample contained in a fission chamber used as a fission tag; instead, a method was developed based on the measurement of gamma multiplicity and full energy deposition.[7] This method enabled us to use a thicker sample and thus helped reduce the uncertainty associated with counting statistics. Using this method both fission and capture reactions were simultaneously measured by the same detector, a feature that removed some of the uncertainties, as described in Sec. III.

I.A. Detection Concept

The goal of this work was to measure the ^{235}U capture cross section from a few electron-volts to ~2 keV with good energy resolution. Methods for direct capture measurement usually detected the capture gamma cascade as an indication for a capture event. In a fissile material this is complicated by emission of gammas from fission events. A traditional way to overcome that problem is to contain the sample in a fission chamber that provides a tag signal when fission occurs; this signal is then used to veto the gamma measurement (see Ref. 6 for example). Another method described in Ref. 8 used a Gd-loaded scintillator to detect capture gammas and the delayed absorption of the neutrons in Gd to detect a fission event. A similar method was also used in Ref. 9 using a different detector geometry.

Reference 10 describes alpha measurements with the Romashka-3 detector. In this work the ratio of capture to fission cross section (alpha) was measured using a high-efficiency segmented gamma detector that surrounds the sample. Fission and capture reactions can be separated based on their observed gamma multiplicity. The multiplicity of fission gammas (peaks at multiplicity 8 to 10) is higher than the multiplicity from a capture gamma cascade (peaks at multiplicity 3 to 4) and was used to separate the two reactions. The difficulty of such methods is treatment of the overlap regions between the multiplicity distributions that span multiplicities 2 through 8. In Ref. 10 alpha values were extracted up to to 32 eV.

The idea in the current work was to explore the possibilities of using a high-efficiency gamma multiplicity detector to distinguish fission from capture events; preliminary results of this work were presented in Ref. 7. Several aspects of the multiplicity detector can help; in order to detect prompt fission gammas with no contribution from capture gammas, the total gamma-cascade energy deposition above the ^{235}U binding energy (~6.55 MeV) was measured. Below this energy both fission and capture gammas were recorded by the detectors; however, the detected multiplicity (related to number of gammas emitted) was higher for a fission event compared to a capture event. Thus, it was possible to correct the mixed data by subtracting the contribution from fission. The difference between the current work and Ref. 10 is that in the current work the total deposited gamma energy was used to separate fission from capture reactions. The gamma multiplicity was used to improve the separation. This method enabled capture and fission yield measurements up to neutron energy of 3 keV; more details are given in Sec. III. In Ref. 5 a fission chamber was used to normalize the measured fission and capture yields, but in the current work the normalization to ENDF/B-VII.1 was done using two different energy regions, described in more detail in Sec. III.

A possible limitation of the current method is sensitivity to fluctuations in the fission gamma cascade as a function of the incident neutron energy. In the method described here, fission was detected by setting a threshold of ~8 MeV for total gamma energy deposition. This fraction of the gamma energy can possibly change as a function of the neutron kinetic energy or resonance spins and can translate to fluctuations in the observed fission cross section. However, this work focused on incident energies below 3 keV, which is a small change in the neutron kinetic energy compared to the binding energy. In addition, for ^{235}U the fission cross section in this range is well known, and the new fission measurement was compared to evaluations to quantify these effects.

II. EXPERIMENTAL SETUP

The present measurement was conducted at Rensselaer Polytechnic Institute (RPI) using the time-of-flight (TOF)

method and the electron linear accelerator (LINAC) at the Gaerttner LINAC Center. The water-cooled tantalum target[11] emitted 6×10^{11} neutrons/s approximately isotropically. A 16-segment NaI(Tl) γ-multiplicity detector located at the 25-m experimental station was used for the measurement. A 5.08-cm-diameter collimated neutron beam passed into the center of the detector through an on-axis cylindrical air gap. The sample location was geometrically centered within the 16 crystal segments at a distance of 25.56 m from the neutron production target. There was a 1.0-cm-thick annular B_4C liner enriched to 99.5 at. % in ^{10}B between the central beam path and the NaI(Tl) segments. The function of this liner was to minimize low-energy neutrons scattering from the sample and then interacting with the detector segments. The details of the multiplicity detector can be obtained from previously published articles.[12,13] Events that passed the required energy thresholds of 300 keV in at least one segment and a total γ energy of 360 keV in the detector were recorded. Each event was categorized with the following tags: TOF channel, multiplicity (1 to 15), and γ energy group (up to four groups). The multiplicity detector is shown in Fig. 1 as a cutaway view displaying the key features of the detector.

The experimental configuration for the LINAC and the data acquisition system were optimized for the desired energy range of the measurement. Considerations included obtaining the desired neutron flux, preventing neutron overlap between LINAC pulses, and resolving the width of the resonances being measured. Experiments in two energy ranges were performed, one covering the range from 0.01 eV to 40 eV
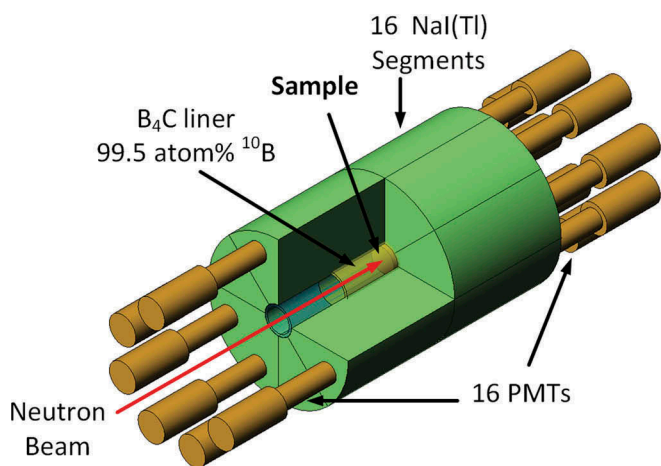
and the other from 10 eV to 3 keV. The low-energy-range experiment was done first because the cross sections of ^{235}U are well known in this energy region and the method could be validated. The experiment in the high-energy range required a correction for scattered neutrons that penetrated the $^{10}B_4C$ liner and were captured in the NaI detector. A correction for these so-called false-capture events was developed and is described in Sec. III.

For the low-energy range the following configuration was selected: enhanced thermal target,[14] 0.125 cm of Pb in beam, a pulse repetition rate of 25 pulses per second, and a pulse (burst) width of 500 ns.

For the high-energy range the following configuration was selected: bare bounce target,[11] 0.3175 cm of Pb and ~0.05 a/b B_4C overlap filter in beam, a pulse repetition rate of 225 pulses per second, and a pulse (burst) width of 15 ns.

II.A. Samples

The samples for the experiment consisted of multiple 1.27-cm- (0.5-in.)-diameter metallic uranium disks enriched to $93.33 \pm 0.03\%$ in ^{235}U with nominal thickness of 0.011 cm. An isotopic analysis was conducted on three representative disks to determine the enrichment, as given in Table I.

Two samples were used for this experiment, as detailed in Table II; for the low-energy experiment a thin sample was needed due to the high fission and capture cross sections of ^{235}U. The low-energy sample included nine discs arranged in a sample can measuring 5.04 cm in diameter. For the high-energy experiment the sample had about eight times larger mass and included nine stacks of eight disks each in the sample can. The arrangement of ^{235}U stacks, wrapped in aluminum foil, in the sample can is shown in Fig. 2. An empty can with an equal amount of aluminum foil was used to measure the background from Al capture.

Fig. 1. Cutaway image of multiplicity detector showing the B_4C liner positioned between the neutron beam path and the 16 NaI segments. Each segment was connected to a photomultiplier tube (PMT). The sample location is in the center of the detector, creating an approximate 4π geometry.

TABLE I

Averaged U Isotopic Enrichment of the Three Disks That Were Assayed

Isotope	Weight Percent
^{234}U	1.087 ± 0.016
^{235}U	93.334 ± 0.034
^{236}U	0.1266 ± 0.0018
^{238}U	5.452 ± 0.021

⊗ANS

TABLE II

The U Samples Used for This Measurement

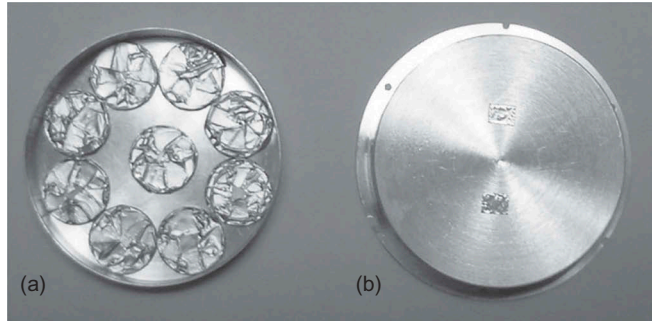| Experiment	Number of U Disks	Mass (g)	Atomic Density (a/b)
Low energy	9	2.4	0.00054 ± 0.00002
High energy	72	18.9	0.00436 ± 0.00002

Fig. 2. A view of the U sample used for the high-energy measurement. (a) Nine stacks of eight disks with a total mass of about 18.9 g of U (see Table II). (b) The cover that closes the aluminum can.
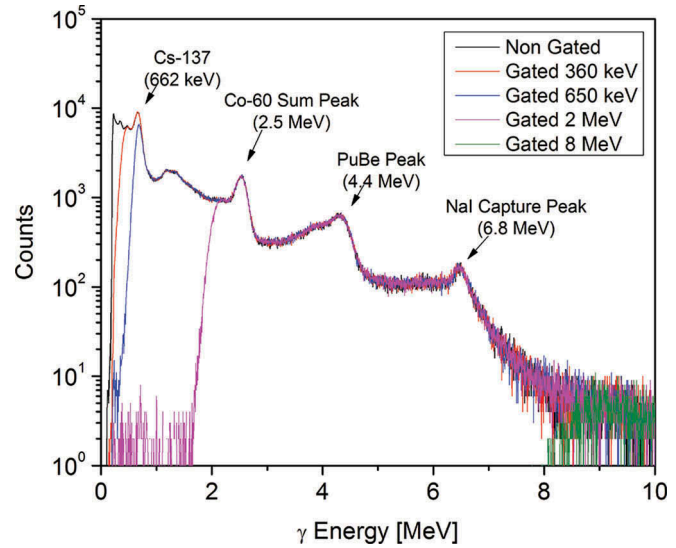

Fig. 3. Gamma calibration spectra recorded as a sum of the 16 segments of the detector; the plot also shows several gated spectra that illustrate different discrimination points that were used for testing.

II.B. Detector Settings

The RPI multiplicity detector is capable of recording the number of segments of the detector that were hit with energy above a threshold (300 keV for this experiment) and provides the total energy deposited in four groups of energy as described in Table III. The detector was energy calibrated using different gamma sources to make sure it covered the whole energy range up to about 12 MeV. An example of the pulse height spectra and several discrimination settings is shown in Fig. 3. These data show good spectroscopic quality for such a large scintillator (resolution of about 11% at the 2.5 MeV ^{60}Co sum peak) and the ability of the system to discriminate at different thresholds when the spectrum was gated by the discriminator output from the detector system.

II.C. Data Collection

For the low-energy experiment about 6.4 h of ^{235}U data and 1.7 h of empty can (background) data were acquired. A 2.54-mm-thick, 98.1 at. % enriched ^{10}B$_4$C sample was measured in order to obtain the neutron energy-dependent flux shape by recording the 478-keV gamma from neutron absorption in ^{10}B. For the high-energy experiment about 25.3 h of ^{235}U data and 4.3 h of empty can (background) data were acquired. The data were collected in multiple files representing about 10 min of data collection each, which facilitated a statistical analysis on the quality of the data and dependence on the neutron beam stability. Three ^{235}U fission detectors recorded neutron beam monitor data at

TABLE III

Detector 4 Energy Group Settings for the Low- and High-Energy Experiments

| Group | Low Energy | | High Energy | |
	Energy (MeV)	Description	Energy (MeV)	Description
1	2 to 4	Capture + fission	<0.36	Discarded
2	4 to 6	Capture + fission	0.36 to 0.6	Scattering
3	6 to 8	Capture + fission	2 to 8	Capture + fission
4	>8	Fission	>8	Fission

an 8-m flight path. These monitors were used for the statistical check (comparing ratios of multiplicity detector count integral to monitor count integral) and also for normalization of the data to ensure fluctuations in neutron production by the LINAC were removed from the data.

III. DATA ANALYSIS

The measured data were saved in multiple files and were subject to statistical analysis to ensure that the multiplicity detector and the beam monitors tracked each other and to identify any anomalous data. If a data set deviated significantly from the other sets it was removed from the analysis. Next the data were dead-time corrected and summed for both the ^{235}U and the empty can samples; this sum preserved the 16 multiplicity in four energy groups as recorded by the detector.

First the low-energy experiment was analyzed by summing the data over the 11.7-eV and 13.4-eV resonances, which are predominately capture and fission, respectively, to obtain the multiplicity distribution. The distributions are plotted in Fig. 4 for different energy groups. For fission events the peak multiplicity at the high-energy bin (corresponding mostly to fission) is about 8, and it decreases as the total gamma energy deposition decreases. Contamination from capture is evident in the 2 to 4 MeV energy group where the multiplicity peaks at 3. For capture events the peak multiplicity is about 4 for the 4 to 8 MeV energy

range. Note that because the 11.7-eV resonance includes a small amount of fission, some nonzero probabilities (peaking at multiplicity 8) are visible in the capture data for the >8 MeV bin. The 2 to 4 MeV bin seems to have similar multiplicity for predominately fission or capture resonances; however, it is an important bin because a large fraction of the counts are in this bin.

For the low-energy experiment, capture rates were calculated by summing multiplicities 1 to 5 for the 2 to 4 MeV and 4 to 6 MeV energy groups. Fission was a sum of multiplicities 5 through 15 in the >8 MeV group. For the high-energy experiment, capture was a sum of all multiplicities from the 2 to 8 MeV group and similarly fission for the >8 MeV group.

In the high-energy experiment the scattering group contained mostly events resulting from scattered neutrons that interacted with the B_4C liner and the subsequent detection of the 478-keV γ ray emitted from the ^{10}B(n,α)^{7}Li* reaction.

Ignoring multiple scattering in the sample, the probability Y_x that interaction x of a neutron of certain energy will occur in the sample, termed the yield, is given by Eq. (1):

$$Y_x = \left(1 - e^{-N\sigma_t}\right)\frac{\sigma_x}{\sigma_t} \ , \tag{1}$$

where

   N = number of atoms per barn in the sample

   σ_x = microscopic cross section for interaction x (x = capture or x = fission)

   σ_t = total microscopic cross section.

Equation (1) is the theoretical yield for an interaction and shows the dependence of the yield on the microscopic cross section. The experimental yield of a particular reaction Y_x^{exp} in each TOF channel was calculated from Eq. (2):

$$Y_x^{exp} = \frac{R_S - R_B}{\phi} \ , \tag{2}$$

Fig. 4. Measured gamma multiplicity distribution of capture and fission obtained from (a) the 13.4-eV and (b) the 11.7-eV resonances in ^{235}U. The counts for each multiplicity were normalized to the multiplicity sum over all energy groups.

where R_S and R_B are the dead-time-corrected, beam-monitor-normalized count rates for the sample and background, respectively, and ϕ is the smoothed, background-subtracted flux shape. The fission yield was calculated by using the experimental data from the fission group and normalizing it to a calculated yield determined from ENDF/B-VII.1 at a particular energy or
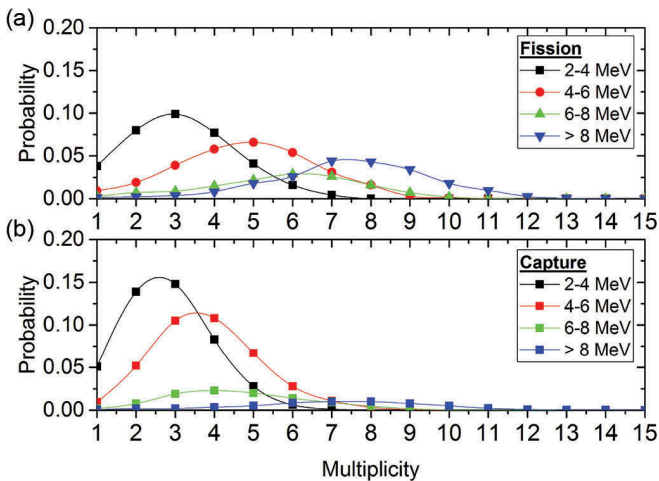
resonance. The fission yield Y_f for all remaining energies was calculated from the experimental yield as shown in Eq. (3):

$$Y_f = k_1 Y_f^{exp} , \qquad (3)$$

where k_1 is a constant that includes the flux normalization and detection efficiency. The present measurement technique for determining the capture yield relies on removing the correct amount of fission events from the capture-fission group. The capture yield was considered as a linear combination of the capture-fission group and the fission group. The expression for the capture yield, Y_γ, is shown in Eq. (4), where k_2 and k_3 are the coefficients for the linear combination:

$$Y_\gamma = k_2 Y_{\gamma f}^{exp} - k_3 k_1 Y_f^{exp} . \qquad (4)$$

The coefficients k_2 and k_3 were found by simultaneously solving Eq. (4) as a system of two equations by using ENDF/B-VII.1 values at two well-known energy regions (or resonances). This method for the simultaneous measurement of the neutron capture and fission cross section was first tested by applying it to the low-energy experiment in the neutron energy range between 0.01 eV and 40 eV. At neutron energies below 600 eV the B$_4$C liner did an excellent job (>99%) of minimizing scattered neutrons reaching the NaI(Tl) segments. As the incident neutron energy increased, the liner efficiency decreased. With the decreasing efficiency of the boron liner, the probability of a scattered neutron passing through the liner and interacting with the γ-multiplicity detector increased. The interaction of concern was a capture event by the iodine in the NaI crystals (shown in Fig. 3 as 6.8 MeV peak). When such a capture event occurred in the detector volume, the emitted γ rays deposited energy in the NaI scintillator and the interaction was detected. When the deposited γ energy was greater than 2 MeV, the event was recorded in the capture-fission energy group. These events were designated as "false capture" and treated as a background in the capture spectra. The removal of this background was represented by including another term in the expression for the capture yield as shown in Eq. (5), where f_c is the false capture fraction and Y_s is the scattering yield:

$$Y_\gamma = k_2 Y_{\gamma f}^{exp} - k_3 k_1 Y_f^{exp} - f_c Y_s . \qquad (5)$$

In most previous capture experiments using the γ-multiplicity detector at RPI, the background from false capture was kept negligible by limiting the incident neutron

energy analyzed to less than 600 eV. The present measurement was the first time that the false capture background was characterized in detail and a process for its removal performed. Since Eq. (5) depends on the scattering yield and this interaction was the most difficult to measure, the scattering yield was replaced by $Y_s = Y_t - Y_\gamma - Y_f$, where the total yield Y_t is the sum of the yields from all interactions. Making the substitution for Y_s in Eq. (5), substituting for Y_f from Eq. (3), combining like terms, and solving for the capture yield in TOF channel i gives the expression shown in Eq. (6):

$$Y_{\gamma_i} = \frac{k_2 Y_{\gamma f_i}^{exp} - (k_3 - f_{c_i}) k_1 Y_{f_i}^{exp} - f_{c_i} Y_{t_i}}{1 - f_{c_i}} . \qquad (6)$$

In Eq. (6), the capture yield is determined as a function of experimental yields from the capture-fission and fission groups, the normalization coefficients, the total yield, and the false capture fraction. The capture yield in Eq. (6) was bounded by the total yield. Since both the fission yield and the total yield for ^{235}U are well known at the energies measured in this experiment, any change in the value of the capture yield should not result in a change in the fission or total yield. This implies that the interaction that was allowed to change was the scattering yield; thus, to keep the evaluated total and fission yield unchanged, a new scattering yield is given by $Y_s = Y_t - Y_f - Y_\gamma$.

The last variable in Eq. (6) that required examination was the false capture fraction f_c. The false-capture fraction was initially investigated by performing simulations with MCNP-Polimi[15] in order to track the γ ray production and energy deposition on a particle-by-particle basis. The simulated, energy-dependent false capture fraction was sensitive to the capture cross sections for iodine and varied depending on the nuclear data evaluation used. In order to improve the analysis, the false capture fraction was examined through experiments with carbon and lead samples. These materials were good samples to experimentally determine the impact of the false capture background because their primary interaction was scattering, their scattering cross sections were generally constant over the energy range of interest, and their capture cross sections were very small. The false capture fraction as a smoothed function of neutron energy is presented in Fig. 5. This function was determined from flux-normalized lead data measured during a separate neutron scattering experiment. The parameters used to collect the lead data were the same as those used for the capture-fission group in the ^{235}U experiment. The false capture fraction
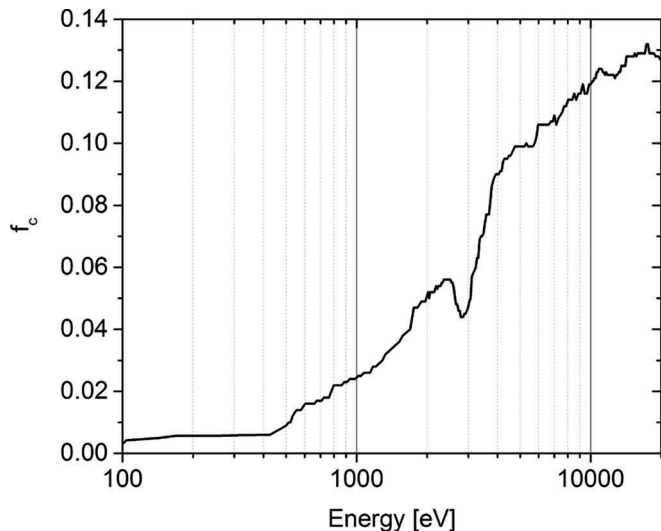
Fig. 5. False capture fraction f_c as a smoothed function of neutron energy. This function represents the fraction of the scattered neutrons that were recorded in the capture-fission energy group. The scattering experiment used the same parameters as the ^{235}U experiment but substituted lead as the sample.

was then used in Eq. (6) to determine the capture yield. As expected, the false capture fraction was less than 1% at neutron energies below 600 eV. At neutron energies near 1 keV, the false capture fraction was 2.5%. The value of f_c continued to increase until it reached a maximum of ~13% at neutron energy of ~18 keV.

It is also important to consider the interaction of the mostly fast fission neutrons with the large NaI detector. These interactions will produce gammas that can be detected. The interaction of the fast neutrons will occur several tens of nanoseconds after a fission event took place and will be within the 500-ns coincidence time of the multiplicity detector. The normalization factor k_3 takes this into account in the fission yield shape subtracted from the capture + fission yield.

IV. RESULTS

A test of the measurement technique was applied to ^{235}U data obtained from an experiment conducted at neutron energies that covered the range of 0.01 to 40 eV. This energy region provided two advantages for a test of the measurement technique: The cross sections for both fission and capture were well known, and the boron liner effectively minimized scattered neutrons entering the detector volume. The fission group (>8 MeV) was normalized at the ENDF/B-VII.1 thermal point energy of 0.0253 eV to determine the constant k_1. From this normalization, the measured fission data were

compared with the calculated yield performed with the shape-fitting code SAMMY 8 (Ref. 16) and ENDF/B-VII.1 (Ref. 2) resonance parameters. Since the samples used in the experiment were not considered thin, a neutron that was initially scattered could have had a secondary interaction within the sample. The SAMMY code accounted for the multiple scattering in the sample and the experimental resolution function effects.

In order to determine the coefficients k_2 and k_3, the thermal point (0.0253 eV) and the area under the 11.7-eV resonance were chosen to normalize the data. This resonance was chosen because it is one of the resonances with lowest contribution from fission. The capture yield was also calculated using SAMMY using ENDF/B-VII.1 resonance parameters, and this calculation was used for the normalization. The measured yield and the calculated yield agree very well, as seen in Figs. 6 and 7.

As a verification of the fission normalization, the integral from 7.8 to 11 eV (recommended by the standards group[17]) was calculated for the fission yield; the ratio of SAMMY calculation to experiment was found to be

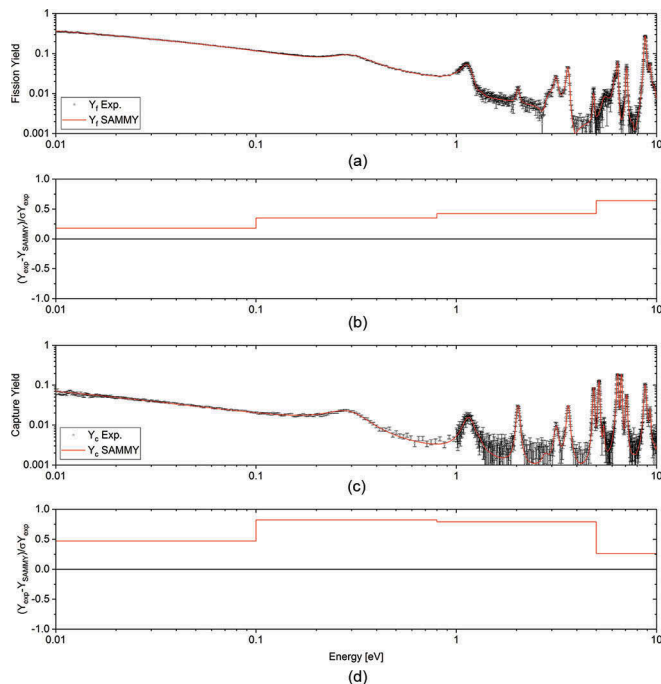

Fig. 6. The graphs depict the excellent agreement between (a) and (b) measured fission and (c) and (d) capture yields and the calculated yields for ^{235}U in the thermal region. The thermal point was used for the normalization of the experimental values. The binned residuals are plotted below each yield plot; the uncertainty used in the residuals plots is dominated by the systematic uncertainty of ~2%.
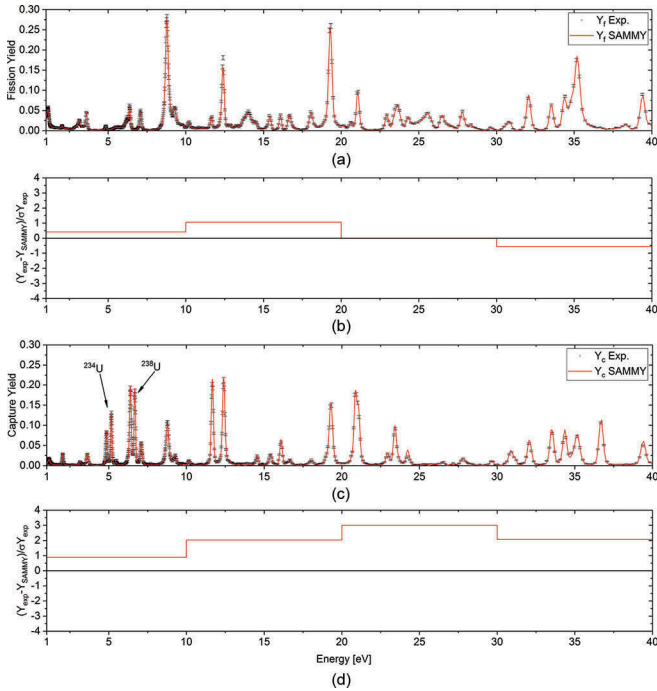
Fig. 7. For both (a) and (b) fission and (c) and (d) capture yields, the plots show good agreement between experimental yields and calculated yields for ^{235}U in the neutron energy range from 1 to 40 eV. The 11.7-eV resonance was used as the second normalization point for the measured capture yield. Resonances from impurities of ^{234,238}U are also shown; they were included in the SAMMY calculation. The residuals in bins of 10 eV are plotted below each yield plot; the uncertainty used in the residuals plots is dominated by the systematic uncertainty of ~2%.

0.98 ± 0.02. The ratio of the integral of the capture experiment and SAMMY yields between 0.0253 eV and 20 eV was found to be 1.00 ± 0.03. The uncertainty of the ratios reflects the systematic normalization uncertainty. These ratios indicate that once the measured fission and capture yields were normalized at the thermal point, they were both in excellent agreement with the ENDF/B-VII.1 evaluation.

The results from the low-energy measurement are an indication that this method works very well and provides accurate fission and capture data using only gammas from fission. The good agreement between experiment and evaluation also shows that, within the accuracy of this measurement, energy-dependent fluctuations in the capture or fission gamma multiplicity and energy spectra were not observed.

Based on the good agreement between measured and calculated yield in the thermal region and low-energy resonances, the technique was extended to measurements at higher energies. The technique was improved with the additional steps for removing the false capture background. The well-known resonances used for the

normalization and determination of the coefficients k_2 and k_3 for the higher energy experiment were 11.7 eV and 19.0 eV. The data were recorded with sufficient energy resolution to clearly resolve the resonance structure in the energy range from 10 eV to 2.25 keV. The result of the fission measurement with a comparison to the SAMMY calculation in the energy range from 400 to 500 eV is presented in Figs. 8a and 8b. The fission measurement showed excellent agreement with the calculation from SAMMY based on ENDF/B-VII.1. The capture measurement and calculation are displayed in Figs. 8c and 8d. The experimental capture yields seem to be in good agreement with the SAMMY calculation but clearly are not as good as the fission yields.

A comparison for a higher energy range from 500 to 700 eV is shown in Fig. 9. While fission is in excellent agreement with the evaluations, the experimental capture result was clearly lower than the calculated yield.

To highlight the differences at higher energies the measured and calculated yield were grouped (averaged) into wide energy bins. To compare the two above the resonance region, MCNP 6.1 (Ref. 18) was used, because
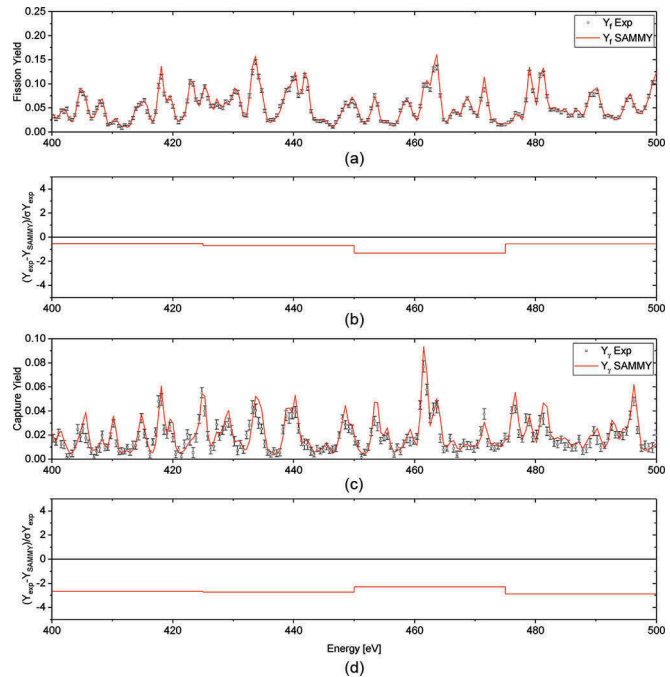

Fig. 8. (a) and (b) Fission and (c) and (d) capture yields for a small energy range compared to the SAMMY calculated fission yield based on ENDF/B-VII.1. The experimental results were in excellent agreement with the calculation for the fission yield and in good agreement with the capture yield. The residuals in bins of 10 eV are plotted below each yield plot; the uncertainty used in the residuals plots is dominated by the systematic uncertainty of ~2% for fission and 3% for capture.
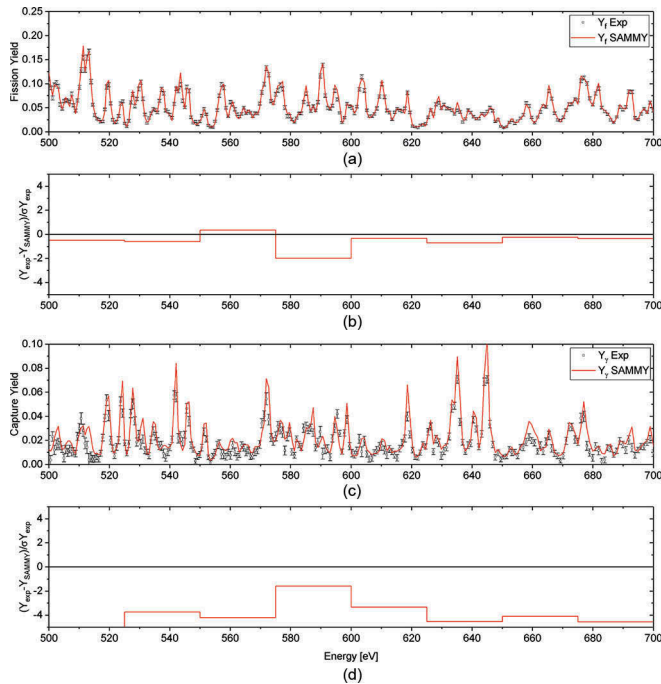
Fig. 9. (a) and (b) Fission and (c) and (d) capture yields from 500 to 700 eV compared to the SAMMY calculated fission yield based on ENDF/B-VII.1. The experimental results were in excellent agreement with the calculation for the fission yield; however, the measured capture yield is lower than the SAMMY calculated yield. The residuals in bins of 25 eV are plotted below each plot; the uncertainty used in the residuals plots is dominated by the systematic uncertainty of ~2% for fission and 3% for capture.

it simulated the multiple scattering and resonance self shielding. The MCNP yield was calculated on the same energy grid as the experiment and SAMMY calculation and was verified to agree with SAMMY below 500 eV. The experiment and calculations are presented in Fig. 10. Yields calculated from the ENDF/B-VII.1 and JENDL-4.0 evaluated libraries were included on the grouped capture and fission yield plots for comparison with the experimental values. The experimental results for the grouped capture yield for ^{235}U were consistently lower than the calculated yield based on ENDF/B-VII.1 in the region between 0.3 and 2.25 keV.

A zoomed plot of the capture yield shown in Fig. 11 illustrates the differences in the energy range of 0.5 to 3 keV. JENDL 4.0 is in good agreement with the experimental data, while the experiment is lower than ENDF/B-VII.1 in the entire region.

IV.A. Uncertainties

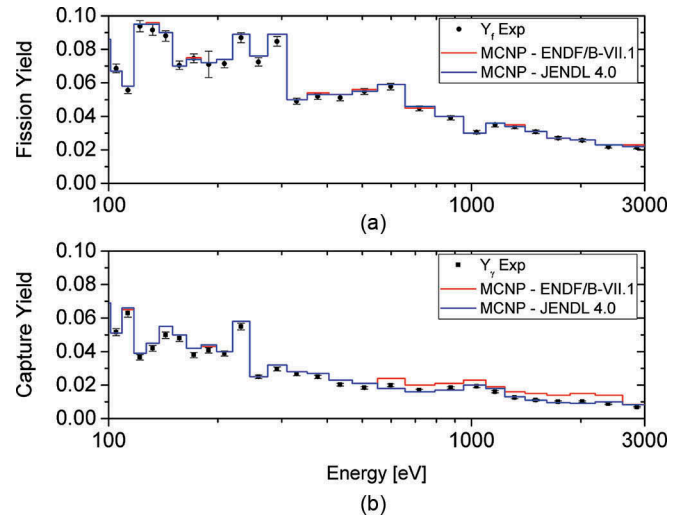There were a number of factors that contributed to the overall uncertainty of the experimental results,

Fig. 10. (a) Grouped fission and (b) capture yields determined experimentally compared to the calculated yields based on both ENDF/B-VII.1 and JENDL-4.0. For fission the agreement is very good; for capture the experimental values generally lie lower than the ENDF/B-VII.1 calculations, in better agreement with the JENDL-4.0 evaluation.
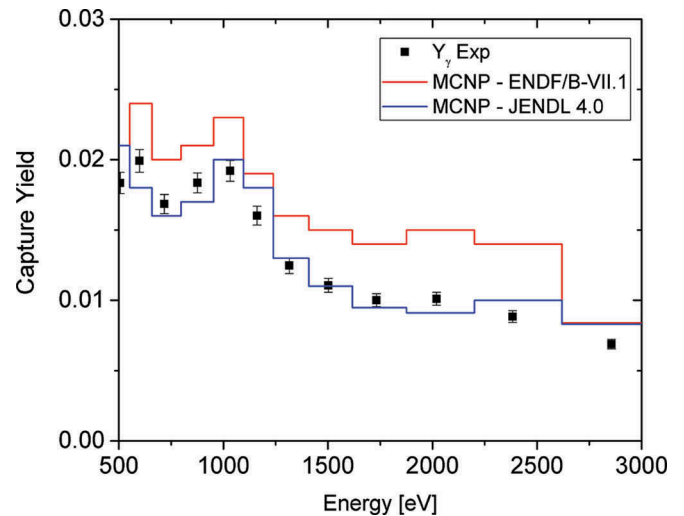

Fig. 11. A zoomed view of the capture yield illustrates the differences between the experiment and evaluations in the energy range from 0.5 to 3 keV.

including counting statistics, normalization values, and the correction for false capture. The plotted experimental uncertainties for the fission and capture yields included the normalization uncertainty. Another source of uncertainty for the high-energy measurement was the false capture correction. An uncertainty of about 30% was estimated and propagated to the uncertainty in the capture yield. The correction itself was about 5% at 1 keV and 40% at 3 keV. The plotted error bars included all the uncertainties in this measurement. The

overall uncertainty is dominated by the normalization uncertainty and was found to be 2% for the fission and low-energy capture yields and 3% for the high-energy capture yield.

It is important to note that simultaneous measurement of the fission and capture yields has several advantages, especially when the fission cross section is well known. The agreement between the measured and calculated fission yield in the resonance region helps to verify the energy resolution function used in analysis. The agreement over the entire energy range from a few electron-volts to 3 keV validates that the flux shape used for the analysis is correct. The yield enhancement due to multiple scattering in the upper kilo-electron-volt region is similar for fission and capture, equals 8% at 500 eV, and reaches 13% near 3 keV; however, it is taken into account by MCNP and SAMMY.

V. SUMMARY AND CONCLUSIONS

The present measurement of the capture yield for [235]U supports a new value for the neutron capture cross section that is lower than the values in ENDF/B-VII.1 in the energy range between 0.6 and 2.25 keV. This observation is similar to results obtained by Jandel et al.[5]

Simultaneous measurements of fission and capture yields help to quantify uncertainties associated with the neutron flux shape, energy resolution, and multiple scattering, which are needed for the analysis and interpretation of the experimental yield.

The use of a high-efficiency gamma detector for this measurement demonstrates that in the case of [235]U the sensitivity of the method to fluctuations in the fission gamma cascade is substantially lower than the uncertainty in the measurement. Such a method enabled us to complete the measurement without the use of a fission chamber.

It will be interesting to attempt this method with [239]Pu, where stronger fluctuations in the gamma cascade might be expected due to larger fluctuations of nubar as a function of the incident neutron energy. An interesting experiment was performed by the LANL group,[19] but a fission detector was used for tagging.

The main limitation of the RPI multiplicity detector is sensitivity to scattered neutrons. The effect was quantified and corrected for; however, as scattering increases with incident neutron energy, the correction becomes larger. This effect prevented extension of the capture measurement above an incident neutron energy of 3 keV. For fission, a gamma energy deposition threshold of 8 MeV was used; thus, false capture events were not recorded, and it was possible to extend the fission yield measurement to energies above 3 keV.

An early version of this data analysis[20] was fitted with SAMMY and was used to form a preliminary evaluation that showed improvements between simulations and experiments of the ZEUS benchmarks[21]; however, a revised evaluation should be used in order to firm the conclusion of Ref. 21. For this early version a uniform uncertainty of 8% was assumed for the capture yield at all energy points. The analysis here uses slightly different data reduction equations and full uncertainty propagation. The main conclusion shown in Fig. 11 remains the same: ENDF/B-VII.1 overpredicts the capture cross section.

To summarize the results, the ratios of evaluation to experimental yield integrals in the energy bin structure of the [235]U fission standard[17] were calculated. To accommodate the URR in JENDL 4.0, which starts at 500 eV, the calculations were done using MCNP. In the resolved resonance region the JENDL 4.0 and ENDF/B-VII resonance parameters are identical. The fission ratios given in Table IV are generally within the experimental uncertainty of 2% of unity, while the capture ratios show deviations that are much larger than the 3% uncertainty of the experiment.

TABLE IV

Ratios of Evaluation to Experimental Yield Integrals*

Enegy (eV)	ENDF/B-VII.1		JENDL 4.0	
	Y_f	Y_c	Y_f	Y_c
0.0253 to 9.4	0.98	1.00	0.98	1.00
7.8 to 11[a]	0.98	1.00	0.98	1.00
9.4 to 150	1.02	1.04	1.02	1.04
150 to 250	1.01	1.06	1.01	1.06
250 to 350	1.03	1.04	1.03	1.04
350 to 450	1.03	1.11	1.03	1.11
450 to 550	1.03	1.16	1.00	1.01
550 to 650	1.01	1.16	1.02	0.87
650 to 750	1.02	1.16	1.03	0.91
750 to 850	1.01	1.15	1.01	0.95
850 to 950	0.98	1.16	0.99	0.97
950 to 1500	1.00	1.23	1.01	1.03
1500 to 2500	1.02	1.48	1.01	1.03

*The uncertainty of the fission and capture yields is 2% and 3%, respectively, with exception of the first two values, where the capture uncertainty is 2%.
[a]For comparison with the standards integral from 7.8 to 11 eV.

Acknowledgments

ORCID

Y. Danon ⓘ http://orcid.org/0000-0001-6187-9731

References

1. N. OTUKA, T. NAKAGAWA, and K. SHIBATA, "Uraniam-235 Neutron Capture Cross Section at keV Energies," *J. Nucl. Sci. Technol.*, **44**, 815 (2007); https://doi.org/10.1080/18811248.2007.9711318.

2. M. CHADWICK et al., *Nucl. Data Sheets*, **112**, 2887 (2011), special issue on ENDF/B-VII.1 Library; https://doi.org/10.1016/j.nds.2011.11.002.

3. K. SHIBATA et al., "JENDL-4.0: A New Library for Nuclear Science and Engineering," *J. Nucl. Sci. Technol.*, **48**, 1 (2011); https://doi.org/10.1080/18811248.2011.9711675.

4. A. SANTAMARINA et al., JEFF Report 22, Nuclear Energy Agency, Organisation for Economic Co-operation and Development (2009).

5. M. JANDEL et al., "New Precision Measurments of the ²³⁵U (*n*, γ) Cross Section," *Phys. Rev. Lett.*, **109**, 202506 (2012); https://doi.org/10.1103/PhysRevLett.109.202506.

6. J. BALIBREA et al., "Measurement of the Neutron Capture Cross Section of the Fissile Isotope ²³⁵U with the CERN n_TOF Total Absorption Calorimeter and a Fission Tagging Based on Micromegas Detectors," *Nucl. Data Sheets*, **119**, 10 (2014); https://doi.org/10.1016/j.nds.2014.08.005.

7. D. WILLIAMS et al., in *Proc. Tenth Int. Topl. Mtg. Nuclear Applications of Accelerators (AccApp 2011)*, Knoxville, Tennessee, 2011, p. 396 (2011).

8. J. C. HOPKINS and B. C. DIVEN, "Neutron Capture to Fission Ratios in U²³³, U²³⁵, Pu²³³," *Nucl. Sci. Eng.*, **12**, 169 (1962); https://doi.org/10.13182/NSE62-A26055.

9. B. C. DIVEN, J. TERRELL, and A. HEMMENDINGER, "Capture-to-Fission Ratios for Fast Neutrons in U²³⁵," *Phys. Rev.*, **109**, 144 (1958); https://doi.org/10.1103/PhysRev.109.144.

10. G. MURADYAN et al., "Multiplicity Spectrometer for Measuring Neutron Cross Sections," *Nucl. Sci. Eng.*, **90**, 60 (1985); https://doi.org/10.13182/NSE85-A17431.

11. M. OVERBERG et al., "Photoneutron Target Development for the RPI Linear Accelerator," *Nucl. Instrum. Methods Phys. Res. A*, **438**, 253 (1999); https://doi.org/10.1016/S0168-9002(99)00878-5.

12. R. BLOCK et al., in *Proc. Int. Conf. Nuclear Data for Science and Technology*, S. IGARASI, Ed., p. 383, Japan Atomic Energy Research Institute (1988).

13. S. WANG et al., "The RPI Multiplicity Detector Response to Gamma-Ray Cascades Following Neutron Capture in ¹⁴⁹Sm and ¹⁵⁰Sm," *Nucl. Instrum. Methods Phys. Res. A*, **513**, 585 (2003); https://doi.org/10.1016/S0168-9002(03)01941-7.

14. Y. DANON, R. BLOCK, and R. SLOVACEK, "Design and Construction of a Thermal Neutron Target for the RPI Linac," *Nucl. Instrum. Methods Phys. Res. A*, **352**, 596 (1995); https://doi.org/10.1016/0168-9002(95)90012-8.

15. S. A. POZZI, E. PADOVANI, and M. MARSEGUERRA, "MCNP-PoliMi: A Monte-Carlo Code for Correlation Measurements," *Nucl. Instrum. Methods Phys. Res. A*, **513**, 550 (2003); https://doi.org/10.1016/j.nima.2003.06.012.

16. N. M. LARSON, "Updated Users' Guide for SAMMY: Multilevel R-Matrix Fits to Neutron Data Using Bayes' Equations," ORNL/TM-9179/R8, Oak Ridge National Laboratory (2008).

17. A. CARLSON et al., "International Evaluation of Neutron Cross Section Standards," *Nucl. Data Sheets*, **110**, 3215 (2009); https://doi.org/10.1016/j.nds.2009.11.001.

18. T. GOORLEY et al., "Initial MCNP6 Release Overview," *Nucl. Technol.*, **180**, 298 (2012); https://doi.org/10.13182/NT11-135.

19. S. MOSBY et al., "Improved Neutron Capture Cross Section of ²³⁹Pu," *Phys. Rev. C*, **89**, 034610 (2014); https://doi.org/10.1103/PhysRevC.89.034610.

20. Y. DANON et al., "Recent Developments in Nuclear Data Measurement Capabilities at the Gaerttner LINAC Center at RPI," *EPJ Web of Conferences*, **111**, 02001 (2016); https://doi.org/10.1051/epjconf/201611102001.

21. L. C. LEAL et al., "²³⁵U Resolved Resonance Evaluation for Benchmark Calculations in the Intermediate Energy Region," *Trans. Am. Nucl. Soc.*, **108**, 495 (2013).